International Journal of Nanoelectronics and Materials
IJNeaM
ISSN 198-5761 | E-ISSN 2232-1535

Shape and Size Dependent Sensing Enhancement by Gold Nanomaterials

Mohamad Danial Hairul Anuar[a], Thangavel Lakshmipriya[b,c], Subash C. B. Gopinath[a,c,*], Tijjani Adam[c,d], Mohammed Mohamme[e], Evan T. Salim[f], and Makram A. Fakhri[g]

[a]*Faculty of Chemical Engineering & Technology, Universiti Malaysia Perlis (UniMAP), 02600 Arau, Perlis, Malaysia*
[b]*Center for Global Health Research, Saveetha Medical College & Hospital, Saveetha Institute of Medical and Technical Sciences, Thandalam, Chennai 602105, Tamil Nadu, India*
[c]*Institute of Nano Electronic Engineering, Universiti Malaysia Perlis (UniMAP), 01000 Kangar, Perlis, Malaysia*
[d]*Faculty of Electronic Engineering & Technology, Universiti Malaysia Perlis, 02600 Arau, Perlis, Malaysia*
[e]*Center of Excellence Geopolymer & Green Technology (CEGeoGTech), Universiti Malaysia Perlis (UniMAP), 02600 Arau, Perlis, Malaysia*
[f]*College of Applied Sciences, University of Technology-Iraq, Baghdad 10066, Iraq*
[g]*College of Laser and Optoelectronics, University of Technology-Iraq, Baghdad 10066, Iraq*

** Corresponding author. Tel.: +601110472006; e-mail: subash@unimap.edu.my*

Received 15 September 2023, Revised 1 October 2025, Accepted 27 October 2025

ABSTRACT

Gold nanomaterials (GNs) of different shapes (nanospheres, nanorods, nanostars) and sizes exhibit properties to enhance the surface area. The surface plasmon resonance of GNs can be tuned by changing their shape and size, which affects the binding efficiency of target antigen and antibody interaction. The shape of GNs can also affect the orientation of attached antibodies and antigens, leading to improved specificity in sensing platforms. This study has investigated the morphological and optical properties of GNs, evaluated the impact of different sizes and shapes on ELISA surfaces, and optimized the conditions to enhance the sensitivity. The morphology and optical properties of GNs were studied using a 3D nanoprofiler and, UV-Visible spectrophotometer. Gold nanospheres (GNPs) with 10, 15 and 30 nm, nanorods with 500,700 and 980 nm, and gold nanostars with 60 nm were employed. Smaller GNPs may have higher binding capacities due to their increased surface area to volume ratio. The height and roughness of anti-spike protein antibody morphology increased when 10 nm GNPs were added, demonstrating attachment between spike-antibody molecules and GNPs. The attained limit of detection (LOD) is 1 pM, where the limit of quantification (LOQ) is 10 pM. Gold nanospheres and nanostars behave better than nanorods and provide good LOD and LOQ.

Keywords: *Nanomaterials, Gold, ELISA, Sensing, Size-dependent*

1. INTRODUCTION

With considerable advancements made in the creation of useful products, the field of nanotechnology has become a popular academic area [1]. Due to their distinctive functional properties and simplicity of manufacture, gold nanomaterials (GNs) have attracted a lot of attention. By altering the nanomaterials' characterization, such as shape, size, and aspect ratio, one may change their intrinsic features, including their optical, electronic, and chemical characteristics [2]. Investigation on the GNs' shape- and size-dependent sensing capabilities offers tremendous commercialization potential. The sensitivity of a given method may be significantly increased by optimizing the choice of GNs based on their size and shape, piquing interest from a variety of industries, including biomedical research, diagnostics, and pharmaceutical development [3]. By enabling the creation of novel assays and diagnostic tools with higher performance and greater detection capabilities, this discovery opens doors for extended applications. GNs are adaptable and may be customized to target certain analytes or biomarkers, which makes them useful for applications in healthcare, environmental monitoring, food safety, and other fields [4,5]. There are a great deal of promises for commercial success and market adoption by resolving the shortcomings of traditional ELISA tests and providing better sensitivity utilizing gold nanoparticles [6,7,8].

While alternative techniques have been developed, they may not always be the best solution, and further research is needed to identify new and innovative ways to enhance the sensitivity of ELISA [9,10]. The development of new detection methods that are tried in this research uses GNs to improve the performance of the assay. We explored the problem of insufficient sensitivity due to the limited surface area of polystyrene in existing ELISA sensing and the need for an improvement. The existing ELISA sensing method is insufficiently sensitive and requires improvement to meet the needs of various applications. The current study is conducting a comprehensive examination to assess the capabilities of three different types of gold nanomaterials, namely gold nanospheres, gold nanorods and gold nanostars, to develop the ELISA using horseradish peroxidase (HRP) enzyme and 3,3',5,5'-tetramethylbenzidine (TMB) substrates to perform enzyme-substrate interactions.

2. EXPERIMENTAL SECTION

2.1. ELISA Procedure

Different concentrations target (COVID-spike protein) were diluted in 5x coating buffer from the BioLegend company for coating on the ELISA plate surface, followed by 24 hours of incubation at 4 °C. To stop the non-specific binding, 2% of BSA was administered to block the ELISA wells for an hour. Each well had the desired dilution of the primary antibody (1:1000) immobilized for two hours. The secondary antibody conjugated HRP was then added, diluted to 1:1000, and incubated for one hour. Using a washing buffer, the washing stages were carried out three times with a 10-minute break in between. Finally, each well was reacted with HRP substrate to examine the interaction between the target and the antibody. A spectrophotometer (Denovix Ds-11 Spectrophotometer, USA) was used to measure the optical density (absorbance) at 450 nm for the substrate.

2.2. Desired Gold Nanomaterials

Gold nanospheres, gold nanorods, and gold nano stars are three different kinds of gold nanomaterials (GNs) purchased. These nanomaterials were selected because of their unique morphologies and characteristics, which may alter how they interact with the target protein and the ELISA surface. In these experiments, gold nanorods with three different sizes from 500, 700, and 980 nm, gold nanospheres with sizes of 10, 15, 30 nm and a nanostar with 60 nm were used. In standard ELISA plates, it has 96 wells, which are named A, B, C, D, E, F, G, and H. In these experiments, we placed A well with coating buffer, B well with 10 fM, C well with 100 fM, D well with 1 pM, E well with 10 pM, F well with 100 pM, G well with 1 nM and H well with 10 nM. We used coating buffer and different concentrations of antigen to find the best concentration to attach gold nanomaterials by amine-gold electrostatic attractions. The absorption spectra of gold nanoparticles were recorded at 520 nm using UV UV-Visible spectrophotometer.

2.3. UV-Visible Spectrophotometer

The characterization of gold nanoparticles by UV UV-visible spectrophotometer (Denovix Ds-11 Spectrophotometer, USA) was carried out at room temperature. Where a small amount of GNs was placed into a 1 cm path length quartz cuvette with water as the reference and measured by a UV-Visible spectrophotometer. Proper calibration of the instrument is crucial to ensure reliable measurements. This calibration process involves using a blank reference, typically a solvent or buffer, to zero the baseline before measuring the samples. To investigate the influences of GNs on the ELISA surface, a series of absorbance measurements was conducted at specific wavelengths.

2.4. Observation under 3D Nano Profiler

The 3D Nano Profiler (WT-250 Series, Hawk 3D Nano-Profiler, Korea) is a type of instrument used for surface measurement and characterization. It is made to deliver very accurate, non-contact measurements of surface topography and roughness at the nanometre scale. The device scans the surface of the sample with a sharp tip using a scanning probe microscopy technology and analyses the height differences between the tip and the surface using laser interferometry or capacitance sensing. The 3D nanoprofiler can measure a wide range of surface features, including step heights, surface roughness, waviness, flatness, and other parameters. It can measure surface features with sub-nanometre resolution and accuracy, making it an important tool in the field of nanotechnology for research and development of nanomaterials and devices.

3. RESULTS AND DISCUSSION

3.1. 3D Nano Profiler: Surface Roughness Analysis

The 3D nano profiler is a type of profilometer that is used to measure the surface morphology of materials at the nanoscale level [11]. When evaluated with the 3D nano profiler, the desired probe 'spike-COVID protein antibody' and coating buffer solution would have a mostly flat surface with little height changes when there were no gold nanospheres present. This is due to the absence of nanoparticles, which would have less surface roughness. Figure 1 shows the 3D of spike-antibody and 10 nm gold nanospheres from top and side views. When evaluated with the 3D nano profiler, the Spike Antibody in buffer well H and 15 nm of gold nanospheres would have mostly roughness and spike peak with more height changes in the presence of gold nanospheres. This is due to the presence of nanoparticles, which significantly increased surface topography or roughness. Since all nanogolds are supposed to have similar surface properties, this study performed 3D nanoprofiler analysis only with gold nanospheres.

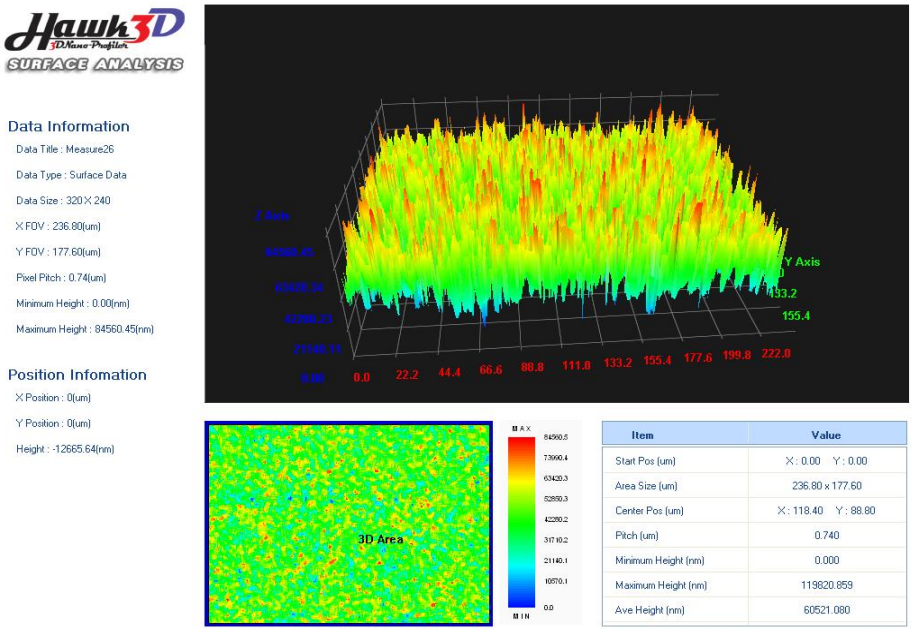

Figure 1. 3D of Spike Antibody in buffer well H and 10 nm of gold nanospheres from the top and side views. Roughness has been measured based on the reference scale provided in the software.

3.2. UV-Visible Spectrophotometer

In ELISA, the absorbance of the coloured product created by the enzymatic interaction between the substrate and the enzyme-conjugated secondary antibody is measured using a spectrophotometer [12]. The sample's concentration of the analyte is inversely proportional to the colour's intensity. The phenomenon known as surface plasmon resonance (SPR) caused more wavelength absorbance of gold nanospheres at 30 nm compared to 10 and 15 nm. The collective oscillation of free electrons in metallic nanoparticles depends on the size, shape, and makeup of the particles. For instance, with gold nanospheres, SPR happens when the incident light coincides with the frequency of the gold nanospheres collective electron oscillation, causing the incident light to be absorbed at a particular wavelength. The gold nanospheres' size and shape determine the peak absorption wavelength, with bigger gold nanospheres exhibiting a redshift and smaller nanoparticles exhibiting a blueshift. As a result, it is conceivable that the variation in peak wavelength (450 nm) absorbance between the 30 nm gold nanosphere sample and the 10 and 15 nm samples is caused by a difference in size or shape, which results in a different SPR frequency.

3.3. Nanomaterial-dependent Enzyme-Linked Immunosorbent Assay

In Figure 2a-c, the colour indicates the concentration-dependency in the ELISA wells with gold nanosphere (nanoparticle). The amount of HRP activity and, consequently, the quantity of the target protein in the sample, are directly inversely correlated with the colour's intensity. Since A well was just coated with coating buffer, any absorbance should not be present based on Figure 2a-c. The target protein was coated in various quantities in the additional wells. The H well, which is anticipated to have the maximum absorbance, was coated with the highest concentration of 10 nM. Figure 3a-c shows UV-Vis absorption peaks in the presence of GNR for a wavelength of 450 nm. A well displays 0.09 absorbance, B well at 0.12 absorbance, C well at 0.14 absorbance, D well at 0.15 absorbance, E well at 0.16 absorbance, F well at 0.19 absorbance, G well at 0.22 absorbance and H well at 0.24 absorbance. The quantity of colour development in each well is shown by the UV-Vis absorption peak at 450 nm, which reflects the level of the enzyme-substrate reaction that took place [13].

Figure 4a shows that the absorbance in wells B through G indicates that there was some enzyme-substrate reaction, with well C showing the largest amount of reaction. The target analyte is aggressively binding to the immobilised capture molecule on the surface of the ELISA plate, as shown by the high absorbance of the H well, which likely contains the largest concentration of the target analyte. This outcome is in line with the normal serial dilution pattern used in the standard ELISA methodology, which allows for the measurement of the concentration of the target analyte in the sample. To make sure that there is no non-specific binding of the detection reagent to the ELISA plate, the A well is employed as a negative control. When the target analyte is absent, the B well serves as a blank to account for any non-specific TMB substrate absorbance [14].

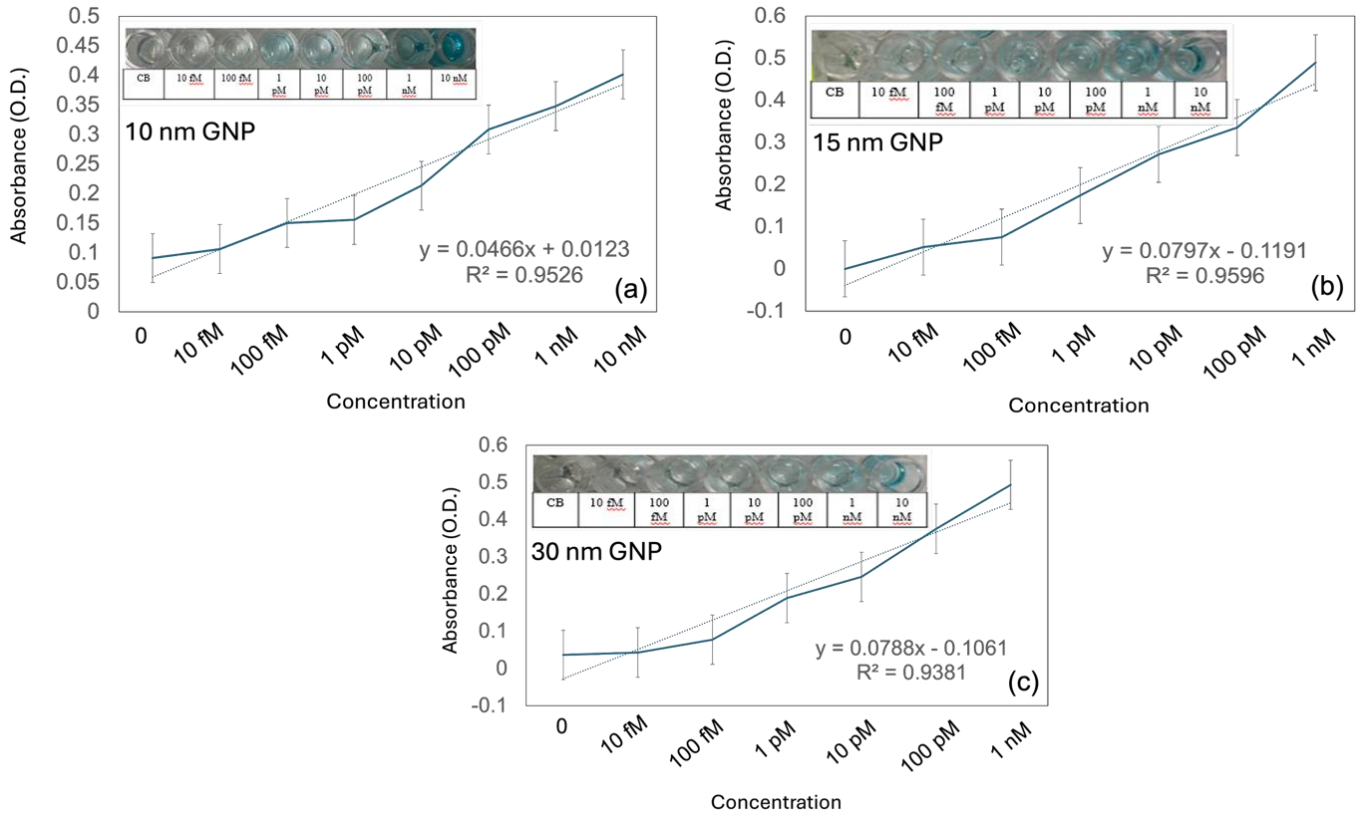

Figure 2. (a) UV-Vis absorption for a 10 nm gold nanosphere. (b) UV-Vis absorption for a 15 nm gold nanosphere. (c) UV Vis absorption for 30 nm gold nanosphere. Figure inserts display the captured images with the ELISA enzyme-substrate reaction. Error values indicate the averaged values from 5 independent experiments.

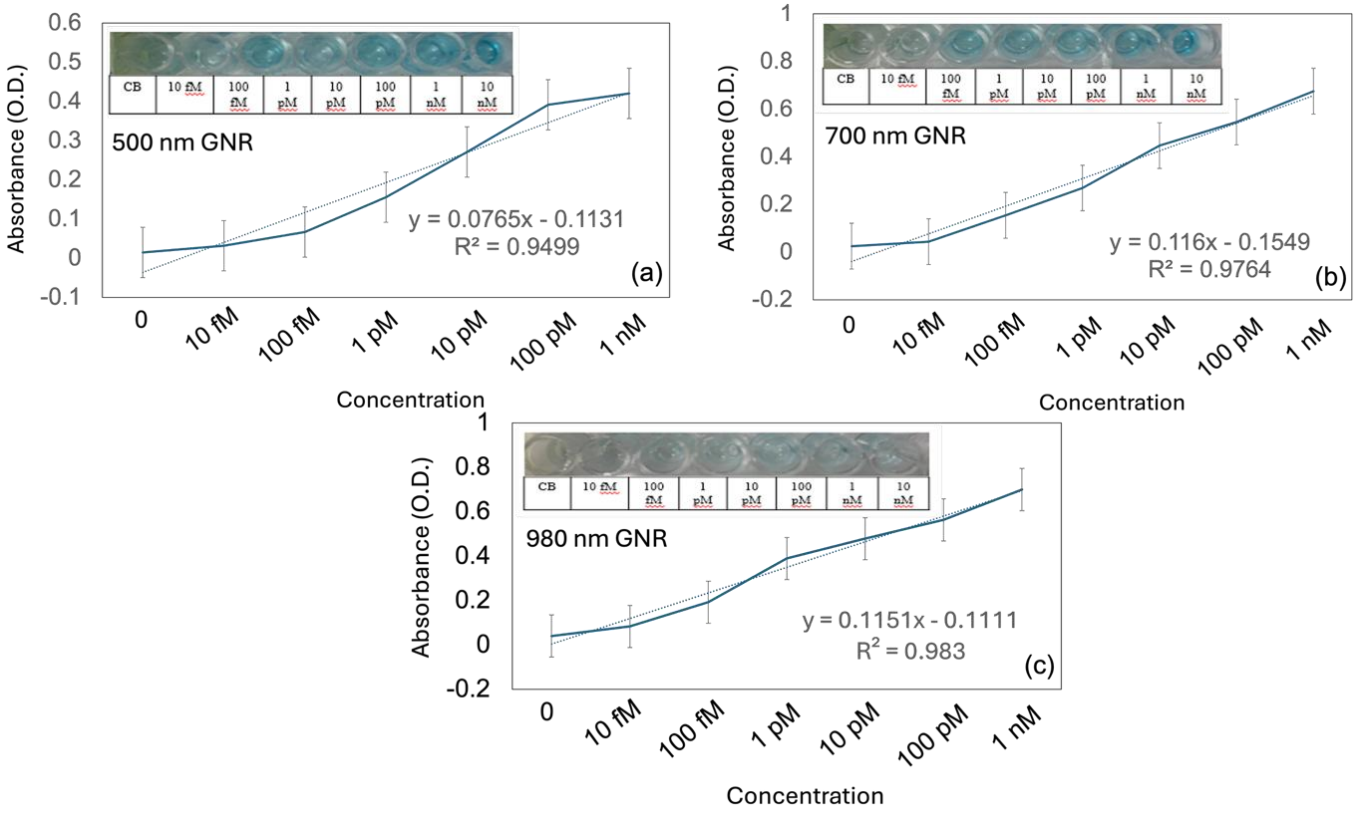

Figure 3. (a) UV-Vis absorption for 500 nm gold nanorods. (b) UV-Vis absorption for 700 nm gold nanorods. (c) UV-Vis absorption for 980 nm gold nanorods. Figure inserts display the captured images with the ELISA enzyme-substrate reaction. Error values indicate the averaged values from 5 independent experiments.

3.4. Effect of Different Sizes and Shapes of Gold Nanomaterials

We evaluated the effects of different sizes and shaped gold nanomaterials which are nanospheres (GNSs), nanorods (GNRs), and nanostars (GNSs) on the ELISA surface. Results above show the rose trend 450 nm absorbance which is A, B, C, D, E, F, and G for various sizes and shapes of GNs. These variations in absorbance at various wavelengths can be traced to GNs' plasmon resonance, which is controlled by the particles' size and shape as well as the surrounding environment. The changes in the synthesis or production of GNs or variations in the ELISA method may be the cause of the variances. The interaction of the GNs with the spike-antibody may cause variations in absorbance at 450 nm, seen in the ELISA. The UV-Vis spectrophotometer measures the plasmon resonance peak at 450 nm and the binding of the GNs may cause this peak to shift. Depending on the concentration of the nanoparticles and antibody, the amplitude of the peak shift may change [17].

3.5. Limit of Detection (LOD) and Limit of Quantification (LOQ) on Gold Nanomaterials Modified ELISA Surfaces

The LOD and LOQ, two crucial parameters in analytical chemistry, are used to establish the lowest concentration of an analyte that can be accurately detected and measured [18–20]. These variables are often evaluated using a variety of analytical methods, such as the widely used ELISA (enzyme-linked immunosorbent test) in biomedical research and diagnostics [15,16]. In the context of ELISA surfaces modified with GNs, the measurement of LOD and LOQ is very important. The sensitivity and detection capacities of ELISA tests are frequently improved using GNs, such as gold nanoparticles or gold nanoclusters. These nanoparticles have special optical and electrical qualities that can magnify the analyte's signal and increase detection limits.

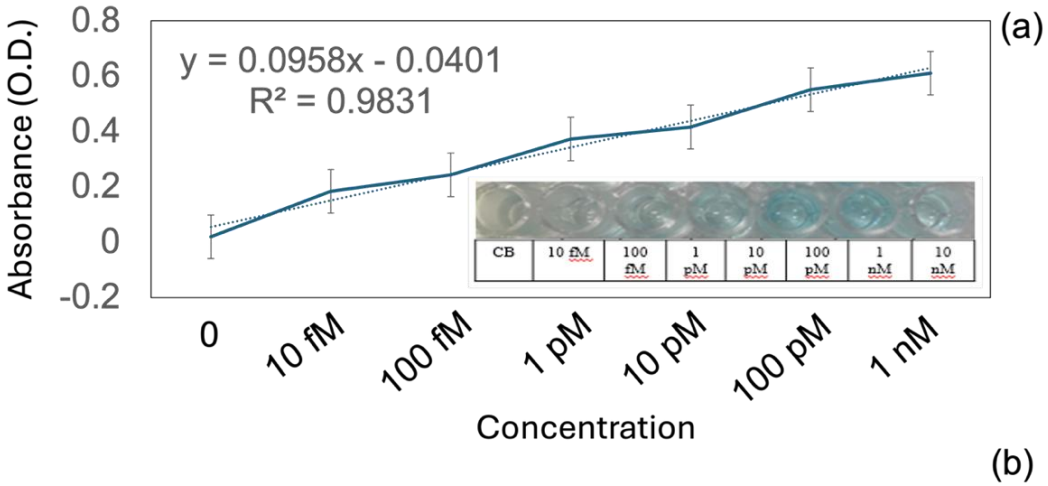

(b)

Nanomaterial	Equation	R^2	Slope	LOD	LOQ
10 nm Nanospheres	y = 0.0466x + 0.0123	0.9526	0.0466	1 pM	10 pM
15 nm Nanospheres	y = 0.0967x - 0.1183	0.9911	0.0967	1 pM	10 pM
30 nm Nanospheres	y = 0.107x + 0.0364	0.9925	0.1070	1 pM	10 pM
500 nm Nanorods	y = 0.1106x -0.0947	0.9965	0.1106	100 pM	1 nM
700 nm Nanorods	y = 0.0975x -0.039	0.9793	0.0975	100 pM	1 nM
980 nm Nanorods	y = 0.1023x -0.0548	0.9863	0.1023	100 pM	1 nM
60 nm Nano star	y = 0.089 x-0.0038	0.9908	0.0890	1 pM	100 pM

Figure 4. (a) UV-Vis absorption for 60 nm gold nanostars. Figure insert displays the captured images with the ELISA enzyme-substrate reaction. Error values indicate the averaged values from 5 independent experiments. (b) Data information gathered from each graph of gold nanomaterials.

Figure 4b shows the data information that was gathered and derived from the graph for each type of GNs. The information stated is the type of GN, equation and regression values that result from the graphs, standard deviation, slope, LOQ and LOD from which we derive the information from calculations based on the equation and regression values. These LOD and LOQ become the indicators to find which concentration suits well for sensing the GNs in ELISA. For all these gold nanoparticles, we conclude that the best sensitivity is at the concentration of 1 pM to 10 nM. These stated concentrations for gold nanoparticles are chosen based on their values in regression values, LOQ and LOD. For regression values, we choose the values that are closer to 1 because they show improved data dependability and correlation. Lastly, for LOQ and LOD, we chose the values that have the lowest analyte concentrations, which were accurately identified and measured. Higher sensitivity and detection abilities are indicated by lower LOD and LOQ values.

CONCLUSIONS

On the ELISA surface, we examined the impact of gold nanomaterials (GNs) in different sizes and shapes, including nanospheres, nanorods, and nanostars. The gold nanospheres had sizes of 10, 15, and 30 nm, the gold nanorods had sizes of 500, 700, and 980 nm and the nanostars (60 nm) were used. Variations in absorbance at 450 nm were seen in the ELISA plate because of the conjugation between the GNs and the spike antibody. The spike-antibody and coating buffer solution displayed a flat surface with minor height fluctuations when tested under a 3D nano profiler in the absence of GNs. The height and roughness of the spike-antibody morphology increased when 10 nm gold nanospheres were added, demonstrating the attachment between the spike-antibody and the GNs. From the information gathered, it was concluded that in the presence of GNs, there are enhanced responses. This is consistent with the common ELISA technology, which uses successive dilutions to gauge the concentration of the target analyte in the samples. The GNs' plasmon resonance, which is controlled by their size, shape, and surroundings, is responsible for the differences in absorbance at various wavelengths. Changes in the synthesis or manufacturing of GNs or modifications to the ELISA procedure may be to blame for discrepancies between different. With all the examined GNs, the best sensitivity was found within the concentration range of 1 pM to 10 nM based on the regression values, limit of quantification (LOQ), and limit of detection (LOD).

REFERENCES

[1] Qiu, Z., Zhang, X., Jia, N., Li, X., et al., 2023. Zeolite nanomaterial-modified dielectrode oxide surface for diagnosing Alzheimer's disease by dual molecular probed impedance sensor. Turkish Journal of Biochemistry, 2023, **48**.

[2] Uhrig, R. E., Loskiewicz-Buczak, A., 1993. Monitoring and Diagnosis of Rolling Element Bearings Using Artificial Neural Networks. IEEE Transactions on Industrial Electronics, 1993, **40**.

[3] Lakshmipriya, T., Horiguchi, Y., Nagasaki, Y., 2014. Co-immobilized poly(ethylene glycol)-block-polyamines promote sensitivity and restrict biofouling on gold sensor surface for detecting factor IX in human plasma. Analyst, 2014, **139**, 3977–3985.

[4] Lee, J., Morita, M., Takemura, K., Park, E. Y., 2018. A multi-functional gold/iron-oxide nanoparticle-CNT hybrid nanomaterial as virus DNA sensing platform. Biosens Bioelectron, 2018, **102**, 425–431.

[5] Mbambo, A. T., Onwubu, S. C., Mdluli, P. S., Madikizela, L. M., 2019. Development of a gold nanomaterial enabled colorimetric sensor method for the analysis of sodium chloride in seawater. Environ Nanotechnol Monit Manag, 2019, **12**.

[6] Ding, Y., Tian, Q., Dong, Y., Xing, L., et al., 2021. Gold-silane complexed antibody immobilization on polystyrene ELISA surface for enhanced determination of matrix Metalloproteinase-9. Process Biochemistry, 2021, **100**, 231–236.

[7] Zhao, J., Chang, W., Liu, L., Xing, X., et al., 2021. Graphene oxide-gold nanoparticle-aptamer complexed probe for detecting amyloid beta oligomer by ELISA-based immunoassay. J Immunol Methods, 2021, **489**, 112942.

[8] Pilely, K., Nielsen, S. B., Draborg, A., Henriksen, M. L., et al., 2020. A novel approach to evaluate ELISA antibody coverage of host cell proteins—combining ELISA-based immunocapture and mass spectrometry. Biotechnol Prog, 2020, **36**, e2983.

[9] Eteshola, E., Balberg, M., 2004. Microfluidic ELISA: On-chip flourescence imaging. Biomed Microdevices, 2004, **6**, 7–9.

[10] Wei, W., Tang, Y., He, H., Gopinath, S. C. B., Wang, L., 2022. Determination of cardiac disease biomarker by plasmonic sandwich ELISA. Biotechnol Appl Biochem, 2022, **69**.

[11] Ramanathan, S., Gopinath, S. C. B., Md. Arshad, M. K., Poopalan, P., 2019. Multidimensional (0D-3D) nanostructures for lung cancer biomarker analysis: Comprehensive assessment on current diagnostics. Biosens Bioelectron, 2019, **141**, 111434.

[12] Chiodo, F., Marradi, M., Tefsen, B., Snippe, H., et al., 2013. High Sensitive Detection of Carbohydrate Binding Proteins in an ELISA-Solid Phase Assay Based on Multivalent Glyconanoparticles. PLoS One, 2013, **8**, 1–11.

[13] Liang, M., Zhang, T., Liu, X., Fan, Y., et al., 2015. Development of an indirect competitive enzyme-linked immunosorbent assay based on the multiepitope peptide for the synchronous detection of staphylococcal enterotoxin A and G proteins in milk. J Food Prot, 2015, **78**.

[14] Fanjul-Bolado, P., Gonzalez-Garcia, M. B. Costa-Garcia, A., 2005. Amperometric detection in TMB/HRP based assay. Bioanalytical chemistry, 2005, **382**, 287–302.

[15] Chen, H., Yang, F., Yin, G., Song, P., 2022. Nanomaterial-assisted determination of osteosarcoma by antibody–osteopontin–aptamer sandwich ELISA. Biotechnol Appl Biochem, 2022, **69**.

[16] Liberelle, B., Merzouki, A., Crescenzo, G. De, 2013. Immobilized carboxymethylated dextran coatings for enhanced ELISA. J Immunol Methods, 2013, **389**, 38–44.

[17] Liu, J. C., Lu, Z. Z., Chen, A. L., 2014. Gold Nanoparticle-Aptamer Based Colorimetric Biosensing Assays. Spectroscopy and Spectral Analysis, 2014, **34**, 2040–2046.

[18] Wei, W., Haruna, S. A., Zhao, Y., Li, H., Chen, Q., 2022. Surface-enhanced Raman scattering biosensor-based sandwich-type for facile and sensitive detection of Staphylococcus aureus. Sens Actuators B Chem, 2022, **364**.

[19] Parihar, A., Ranjan, P., Sanghi, S. K., Srivastava, A. K., Khan, R., 2020. Point-of-Care Biosensor-Based Diagnosis of COVID-19 Holds Promise to Combat Current and Future Pandemics. ACS Appl Bio Mater, 2020, **3**, 7326–7343.

[20] Snehi, V., Verma, H., Pathak, D., 2022. Telemedicine and Biosensors, A Boon in COVID Era: An Update. International Journal of Research and Review, 2022, **9**.